

Using the Extragalactic Gamma-Ray Background to Constrain the Hubble Constant and Matter Density of the Universe

HOUDUN ZENG¹ AND DAHAI YAN^{2,3,4}

¹Key Laboratory of Dark Matter and Space Astronomy, Purple Mountain Observatory, Chinese Academy of Sciences, Nanjing 210008, China; zhd@pmo.ac.cn

²Key Laboratory for the Structure and Evolution of Celestial Objects, Yunnan Observatories, Chinese Academy of Sciences, Kunming 650216, China; yandahai@ynao.ac.cn

³Center for Astronomical Mega-Science, Chinese Academy of Sciences, 20A Datun Road, Chaoyang District, Beijing 100012, China

⁴Department of Astronomy, Key Laboratory of Astroparticle Physics of Yunnan Province, Yunnan University, Kunming 650091, China

ABSTRACT

The attenuation produced by extragalactic background light (EBL) in γ -ray spectra of blazars has been used to constrain the Hubble constant (H_0) and matter density (Ω_m) of the Universe. We propose to estimate H_0 and Ω_m using the well measured >10 GeV extragalactic γ -ray background (EGB). This suggestion is based on the facts that the >10 GeV EGB is totally explained by the emissions from blazars, and an EBL-absorption cutoff occurs at ~ 50 GeV in the EGB spectrum. We fit the >10 GeV EGB data with modeled EGB spectrum. This results in $H_0 = 64.9_{-4.3}^{+4.6}$ km s⁻¹ Mpc⁻¹ and $\Omega_m = 0.31_{-0.14}^{+0.13}$. Note that the uncertainties may be underestimated due to the limit of our realization for EBL model. H_0 and Ω_m are degenerate in our method. Independent determination of Ω_m by other methods would improve the constraint on H_0 .

Keywords: galaxies: jets - gamma rays: galaxies - gamma rays: diffuse background - cosmology: observations

1. INTRODUCTION

A precise and accurate measurement of the Hubble constant (H_0) would provide deep understanding of fundamental physics questions. Multiple paths to independent estimates of H_0 are needed in order to access and control its systematic uncertainties (Suyu et al. 2012).

Gamma-ray astronomy provides a new approach to estimate H_0 (Salamon et al. 1994; Mannheim 1996). The optical depth of the γ -ray photons emitted by extragalactic objects, $\tau_{\gamma\gamma}$, scales as $n_{\text{EBL}}\sigma_{\text{T}}l$, where n_{EBL} is the photon density of the extragalactic background light (EBL), σ_{T} is the Thomson cross section, and l is the distance from the γ -ray source to Earth. l is inversely proportional to H_0 , and n_{EBL} also depends on H_0 . Therefore, through determining the optical depth $\tau_{\gamma\gamma}$, one can estimate H_0 .

Such an approach has been pursued by latter studies. With simulated TeV spectra of blazars, Blanch & Martinez (2005) studied the possibility of using γ -ray absorption to constrain cosmological parameters. Using the EBL density based on galaxy counts, Barrau et al. (2008) derived $H_0 > 74$ km s⁻¹ Mpc⁻¹ at the 68% confidence level, from the TeV spectrum of Mrk 501. With the cosmic γ -ray horizon extracted

from multiwavelength observations of TeV blazars (Domínguez et al. 2013), Domínguez & Prada (2013) derived $H_0 = 71.8_{-5.6}^{+4.6}$ (stat) $_{-13.8}^{+7.2}$ (syst) km s⁻¹ Mpc⁻¹. Biteau & Williams (2015) derived $H_0 = 88 \pm 13$ (stat) ± 13 (syst) km s⁻¹ Mpc⁻¹ by analyzing 106 TeV spectra of 38 blazars. The *Fermi* Large Area Telescope (*Fermi*-LAT) observations of blazars provide good determinations of $\tau_{\gamma\gamma}$ (Abdollahi et al. 2018). Using $\tau_{\gamma\gamma}$ measured from *Fermi*-LAT GeV spectra (Abdollahi et al. 2018) and TeV spectra (Desai et al. 2019), Domínguez et al. (2019) derived $H_0 = 68.0_{-4.1}^{+4.2}$ km s⁻¹ Mpc⁻¹ and $\Omega_m = 0.17_{-0.08}^{+0.07}$ with the combination of the EBL models of Finke et al. (2010) and Domínguez et al. (2011). The constraint on H_0 from γ -ray attenuation has been significantly improved in the past ten years.

The above constraints on H_0 are all derived from point sources. Here, we propose to constrain H_0 and Ω_m using the extragalactic γ -ray background (EGB). The EGB spectrum has been well measured from 0.1 GeV to ~ 800 GeV by the *Fermi*-LAT. This spectrum can be described by a power law with a photon index of 2.32 that is exponentially cut off at ~ 50 GeV (Ackermann et al. 2015). The cutoff is caused by the EBL absorption (Ajello et al. 2015). Similar to the idea proposed by Salamon et al.

(1994), the γ -ray absorption in the EGB spectrum could also be used to constrain the cosmological parameters.

EGB is dominated by the emission of γ -ray blazars (Ajello et al. 2015; Ackermann et al. 2016). With the source count distribution of hard-spectrum blazars, Ackermann et al. (2016) estimated that blazars can explain almost the totality ($86_{-14}^{+16}\%$) of the >50 GeV EGB. In particular, the calculation performed with improved luminosity function (LF) and modeling of the spectral energy distributions (SEDs) of blazars showed that blazars account for the totality of the ≥ 10 GeV EGB (Ajello et al. 2015). Besides, modeling of the EGB spectrum also depends on H_0 . Therefore, we can use the above information to constrain H_0 and Ω_m .

2. METHOD

2.1. Calculation of the EGB spectrum

We follow Ajello et al. (2015) to compute the EGB spectrum contributed by blazars,

$$F_{\text{EGB}}(E_\gamma) = \int_{\Gamma_{\min}=1.0}^{\Gamma_{\max}=3.5} d\Gamma \int_{z_{\min}=10^{-3}}^{z_{\max}=6} dz \times \int_{L_\gamma^{\min}=10^{43}}^{L_\gamma^{\max}=10^{52}} dL_\gamma \cdot \Phi(L_\gamma, z, \Gamma) \cdot \frac{dN_\gamma}{dE} \cdot \frac{dV}{dzd\Omega} \quad (1)$$

$$\times [\text{ph cm}^{-2}\text{s}^{-1}\text{sr}^{-1}\text{GeV}^{-1}],$$

where the LF, $\Phi(L_\gamma, z, \Gamma)$ (at redshift z , for sources of γ -ray luminosity L_γ), is described as a broken power law multiplied by the photon index distribution $\frac{dN}{d\Gamma}$ (Equation (1) in Ajello et al. 2015). The γ -ray spectrum of each blazar, $\frac{dN_\gamma}{dE}$, is modeled as a broken power law (Equation (11) in Ajello et al. 2015). $\frac{dV}{dzd\Omega}$ is the comoving volume element per unit redshift and unit solid angle, which is written as,

$$\frac{dV}{dzd\Omega} = \frac{cd_L^2}{H_0(1+z)^2} \frac{1}{E(z)}, \quad (2)$$

where $E(z) = [\Omega_\Lambda + \Omega_m(1+z)^3]^{1/2}$, $\Omega_\Lambda = 1 - \Omega_m$ in a flat Λ CDM cosmology, and d_L is the luminosity distance.

2.2. Absorption of γ -rays

The optical depth of the γ -ray photons emitted at redshift z as a function of observed γ -ray photon energy, E_γ , is calculated by (e.g., Razzaque et al. 2009)

$$\tau_{\gamma\gamma}(E_\gamma, z) = c\pi r_e^2 \frac{m_e^4 c^8}{E_\gamma^2} \int_0^z \frac{dz_1}{(1+z_1)^2} \left| \frac{dt}{dz_1} \right| \times \int_{\frac{m_e^2 c^4}{E_\gamma(1+z_1)}}^\infty d\epsilon_1 \frac{\epsilon_1 u_{\text{EBL}}(\epsilon_1, z_1)}{\epsilon_1^4} \bar{\varphi}(s_0), \quad (3)$$

where $\left| \frac{dt}{dz_1} \right| = \frac{1}{H_0(1+z_1)E(z_1)}$, $s_0 = E_\gamma \epsilon_1 (1+z_1)/m_e^2 c^4$, and $\bar{\varphi}(s_0)$ is adopted from Gould & Shröder (1967). We use the model of Razzaque et al. (2009) to calculate the comoving EBL density,

$$\epsilon u(\epsilon, z) = (1+z)^4 \epsilon^2 \mathcal{N} \int_z^\infty dz'' \left| \frac{dt}{dz''} \right| \psi(z'') \times \int_{M_{\min}}^{M_{\max}} dM \left(\frac{dN}{dM} \right) \times \int_{z_d(M, z')}^{z''} dz' \left| \frac{dt}{dz'} \right| f_{\text{esc}}(\epsilon') \frac{dN(\epsilon', M)}{d\epsilon' dt} (1+z'), \quad (4)$$

where $\psi(z)$ is the star formation rate (SFR) in unit of $M_\odot \text{ yr}^{-1} \text{ Mpc}^{-3}$, $\frac{dN}{dM}$ is the initial mass function (IMF), $f_{\text{esc}}(\epsilon)$ is the escape fraction of photons from the host galaxy, and $\frac{dN(\epsilon, M)}{d\epsilon dt}$ is the total number of photons emitted from a star. The normalization is determined by $\mathcal{N}^{-1} = \int_{M_{\min}}^{M_{\max}} dM (dN/dM) M$. $z_d(M, z)$ is the redshift of the star (born at redshift z) that had evolved off the main sequence. See Razzaque et al. (2009) for more details.

The uncertainties in modeling the EBL density primarily come from SFR and IMF. We adopt the *Models B* and *C* in Razzaque et al. (2009). Both models use the same SFR (Cole et al. 2001; Hopkins & Beacom 2006), but different IMFs. *Model B* uses Salpeter A IMF (Salpeter 1955), and *Model C* uses Baldry-Glazebrook IMF (Baldry & Glazebrook 2003).

Note that the EBL model of Razzaque et al. (2009) only includes the contribution from starlight. This underestimates the EBL density below 1 eV (Finke et al. 2010), and consequently underestimates $\tau_{\gamma\gamma}$ above $0.3/(1+z)$ TeV.

2.3. Verification of our calculations

We calculate the contribution to the EGB from blazars with the pure luminosity evolution (PLE) LF in Ajello et al. (2015) and the EBL *Models B* and *C*. The parameters in Table 1 in Ajello et al. (2015) are used. Here we adopt $H_0 = 67 \text{ km s}^{-1} \text{ Mpc}^{-1}$ and $\Omega_m = 1 - \Omega_\Lambda = 0.3$, same as that in Ajello et al. (2015). The results are shown in Fig. 1. One can see that EGB above 100 GeV can be explained by the emission from the blazars below the redshift of 0.8, whereas EGB between 10 GeV and 100 GeV can be explained by the blazars below the redshift of 1.5.

We compare our results with Ajello et al. (2015) who adopted the EBL model of Finke et al. (2010). We found that our results are almost the same as that in Ajello et al. (2015) (see their Fig. 3) below 300 GeV. Above 300 GeV, the intensity that we calculated with EBL *Model C*

is higher than the one in [Ajello et al. \(2015\)](#). This is due to our underestimation of the EBL intensity. However, we note that above 300 GeV, the intensity in [Ajello et al. \(2015\)](#) agrees with ours within the errors of the data points.

The results in [Fig. 1](#) show two points: (1) the emission from blazars could be used to explain the EGB above ~ 10 GeV; (2) the difference between EBL models of [Razzaque et al. \(2009\)](#) and [Finke et al. \(2010\)](#) has little impact on explaining the origins of EGB.

3. RESULTS

Calculations of LF and SFR depend on the measurements of H_0 and Ω_m . [Ajello et al. \(2015\)](#) constructed the LF with $H_0 = 67$ km s $^{-1}$ Mpc $^{-1}$ and $\Omega_m = 0.3$. In our purpose, the LF should be modified with different cosmological parameters. Therefore, the LF in Equation (1) is,

$$\begin{aligned} & \Phi(L_\gamma, z, \Gamma) dL_\gamma dz d\Gamma \\ &= \Phi_{\text{Ajello15}}(L_\gamma, z', \Gamma') \frac{dV/dz/d\Omega}{dV'/dz'/d\Omega'} dL_\gamma dz' d\Gamma'. \end{aligned} \quad (5)$$

The SFR in Equation (4) is modified as (e.g., [Domínguez et al. 2019](#)),

$$\psi(z) = \psi_{\text{HB06}}(z') \frac{H_0 E(z)}{H'_0 E'(z)}. \quad (6)$$

The primed quantities are computed with $H'_0 = 67$ km s $^{-1}$ Mpc $^{-1}$ for the LF, and $H'_0 = 70$ km s $^{-1}$ Mpc $^{-1}$ for the SFR, and $\Omega'_m = 0.3$.

3.1. Dependence on H_0

Calculations of both the intrinsic EGB spectrum and $\tau_{\gamma\gamma}(E, z)$ depend on H_0 and Ω_m . In [Fig. 2](#), we can see that the intrinsic spectrum strongly relies on H_0 , especially at the energies below 100 GeV (left panel; H_0 is fixed to 67 km s $^{-1}$ Mpc $^{-1}$ in the calculation of the optical depth); and the dependence of $\tau_{\gamma\gamma}(E, z)$ on H_0 occurs at the energies above 100 GeV (right panel; H_0 is fixed to 67 km s $^{-1}$ Mpc $^{-1}$ in the calculation of the intrinsic EGB spectrum).

3.2. Fitting results

We use the modeled EGB spectrum to fit the >10 GeV observed data. H_0 and Ω_m are set to free, and the other parameters are fixed to those in [Ajello et al. \(2015\)](#) and in [Razzaque et al. \(2009\)](#). The Markov Chain Monte Carlo (MCMC) technique is used to perform our fitting. More details of our MCMC method can be found in [Yan et al. \(2013\)](#).

[Fig. 3](#) shows the best-fitting results with EBL *Model B*. We obtain $H_0 = 72^{+10}_{-9}$ km s $^{-1}$ Mpc $^{-1}$ and $\Omega_m =$

$0.23^{+0.14}_{-0.13}$ ¹. In the fitting, H_0 is anti-correlated with Ω_m (see the 2D confidence contours of the parameters in the right panel), which is consistent with the result obtained by using the EBL model of [Finke et al. \(2010\)](#) in [Domínguez et al. \(2019\)](#). We note that the calculated EGB spectrum below 5 GeV is more sensitive to H_0 and Ω_m (see the solid and dashed lines in the left panel of [Fig. 3](#)). This effect is brought by the LF.

[Fig. 4](#) shows the best-fitting results with EBL *Model C*. We obtain $H_0 = 63.1^{+6.2}_{-4.7}$ km s $^{-1}$ Mpc $^{-1}$ and $\Omega_m = 0.44^{+0.13}_{-0.19}$. The uncertainties on H_0 are at the 9% level. Again, there is a strong degeneracy between H_0 and Ω_m in this model. The EGB spectrum calculated with $H_0 = 67$ km s $^{-1}$ Mpc $^{-1}$ and $\Omega_m = 0.3$ is almost same with the best-fitting EGB spectrum.

Supposing that the two EBL models are equally possible, we derived the combined results in [Fig. 5](#) of $H_0 = 64.9^{+4.6}_{-4.3}$ km s $^{-1}$ Mpc $^{-1}$ and $\Omega_m = 0.31^{+0.13}_{-0.14}$.

4. DISCUSSION AND CONCLUSIONS

We simultaneously constrain H_0 and Ω_m via fitting the > 10 GeV EGB spectrum. Two EBL models are adopted to investigate their impacts on the constraints. The EBL *Model B* in [Razzaque et al. \(2009\)](#) leads to $H_0 = 72^{+10}_{-9}$ km s $^{-1}$ Mpc $^{-1}$ and $\Omega_m = 0.23^{+0.14}_{-0.13}$, and the EBL *Model C* in [Razzaque et al. \(2009\)](#) leads to $H_0 = 63.1^{+6.2}_{-4.7}$ km s $^{-1}$ Mpc $^{-1}$ and $\Omega_m = 0.44^{+0.13}_{-0.19}$. The constraints obtained by using the two EBL models are consistent. The combined results are $H_0 = 64.9^{+4.6}_{-4.3}$ km s $^{-1}$ Mpc $^{-1}$ and $\Omega_m = 0.31^{+0.13}_{-0.14}$. Our constraints are mainly given by the blazars below the redshift of 1.5 (see [Fig. 1](#)).

Using the latest γ -ray attenuation data obtained from γ -ray spectra of blazars, [Domínguez et al. \(2019\)](#) obtained $H_0 = 71.0^{+2.7}_{-2.6}$ km s $^{-1}$ Mpc $^{-1}$ and $\Omega_m = 0.21 \pm 0.06$ with the EBL model of [Finke et al. \(2010\)](#), and $H_0 = 65.0 \pm 2.9$ km s $^{-1}$ Mpc $^{-1}$ and $\Omega_m = 0.14 \pm 0.06$ with the EBL model of [Domínguez et al. \(2011\)](#). Their combined results are $H_0 = 68.0^{+4.2}_{-4.1}$ km s $^{-1}$ Mpc $^{-1}$ and $\Omega_m = 0.17^{+0.07}_{-0.08}$. Our results are in agreement with theirs.

The uncertainties on H_0 are comparable with those obtained by [Domínguez et al. \(2019\)](#). There is a clear degeneracy between H_0 and Ω_m in our calculation. Measurement of Ω_m using other independent methods would improve the constraint on H_0 .

We choose the two easily calculated EBL models to examine the uncertainties introduced by the EBL models. Actually, these two models belong to the same method-

¹ We here report the posterior probability means for the parameters.

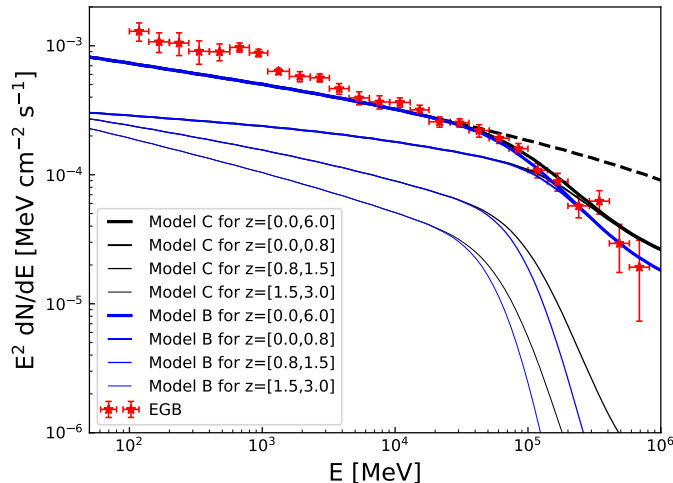


Figure 1. Contribution to the EGB from blazars, calculated with the PLE LF in Ajello et al. (2015) and the EBL models in Razzaque et al. (2009)(solid lines). The dashed line is the one without EBL absorption. Data points are from Ackermann et al. (2015).

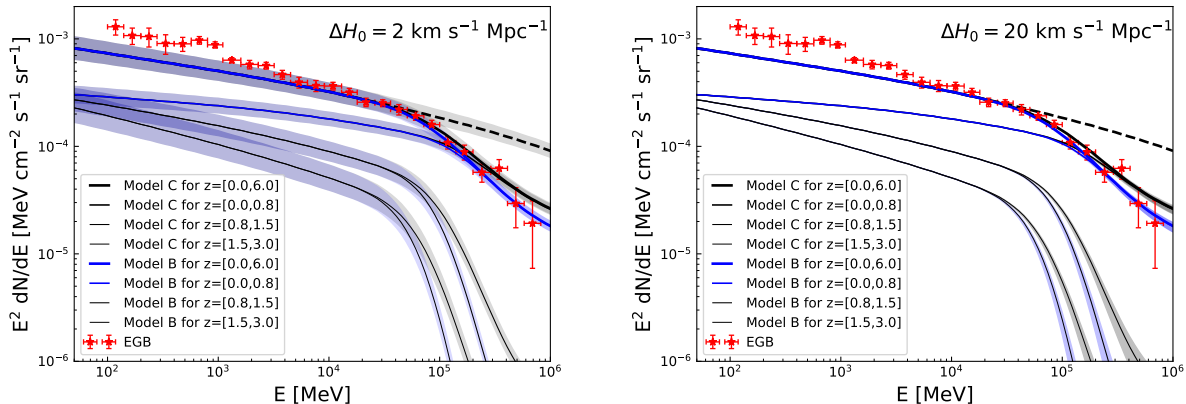


Figure 2. Dependence on H_0 . The results are produced by fixing $\Omega_m = 0.3$. *Left:* H_0 is varied from $65 \text{ km s}^{-1} \text{ Mpc}^{-1}$ to $69 \text{ km s}^{-1} \text{ Mpc}^{-1}$ in the calculation of the intrinsic EGB spectrum. *Right:* H_0 is varied from $47 \text{ km s}^{-1} \text{ Mpc}^{-1}$ to $87 \text{ km s}^{-1} \text{ Mpc}^{-1}$ in the calculation of $\tau_{\gamma\gamma}(E, z)$.

ology, i.e., the physically motivated model. These two models use the same assumption for SFR, and only differ in IMFs. Different assumptions for SFR may introduce extra uncertainties on H_0 . In addition, we cannot examine the uncertainties introduced by different methodologies of building EBL models (e.g., Domínguez et al. 2019). The uncertainties in our results mainly come from EBL models. Therefore, we may underestimate the uncertainties in our results.

Currently, the values of H_0 measured from type Ia supernovae and from cosmic microwave background radiation (CMB) are discrepant at 3σ (Riess et al. 2018). Alternative methods of measuring the Hubble constant,

like the method presented here, is helpful to understand this discrepancy.

ACKNOWLEDGEMENTS

We thank the referee for the constructive comments. We acknowledge financial supports from the National Natural Science Foundation of China (NSFC-11703094, NSFC-U1738124, NSFC-11803081, NSFC-11573060, and NSFC-11661161010) and the joint foundation of Department of Science and Technology of Yunnan Province and Yunnan University [2018FY001(-003)]. The work of D. H. Yan is also supported by the CAS ‘‘Light of West China’’ Program and Youth Innovation Promotion Association.

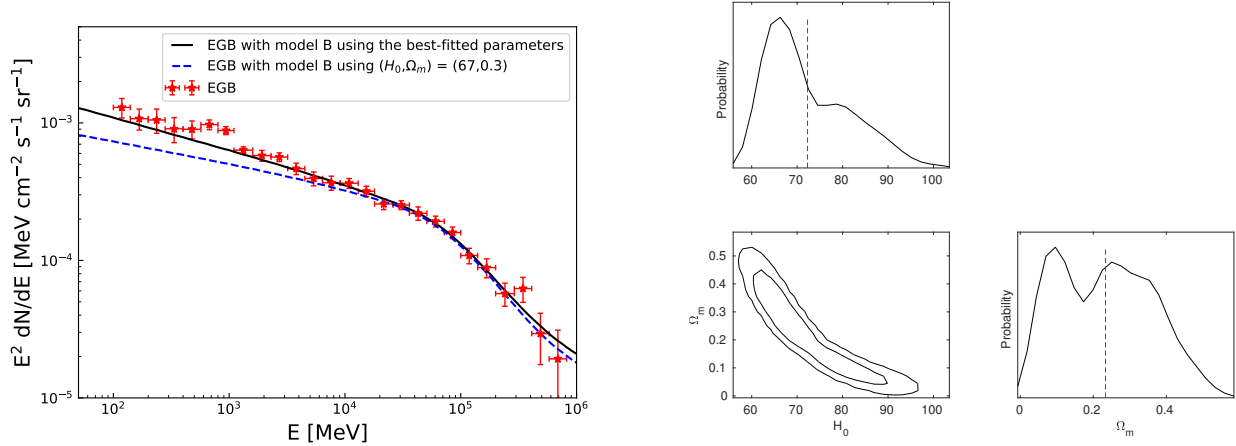


Figure 3. Fitting results with the EBL *Model B*. *Left*: best-fitting to the EGB spectrum above 10 GeV (solid line), and the result calculated with $H_0 = 67 \text{ km s}^{-1} \text{ Mpc}^{-1}$ and $\Omega_m = 0.3$ (dashed line). *Right*: 1D marginalized probability distribution and 2D confidence contours of the parameters, and the dashed line represents the mean of the parameter.

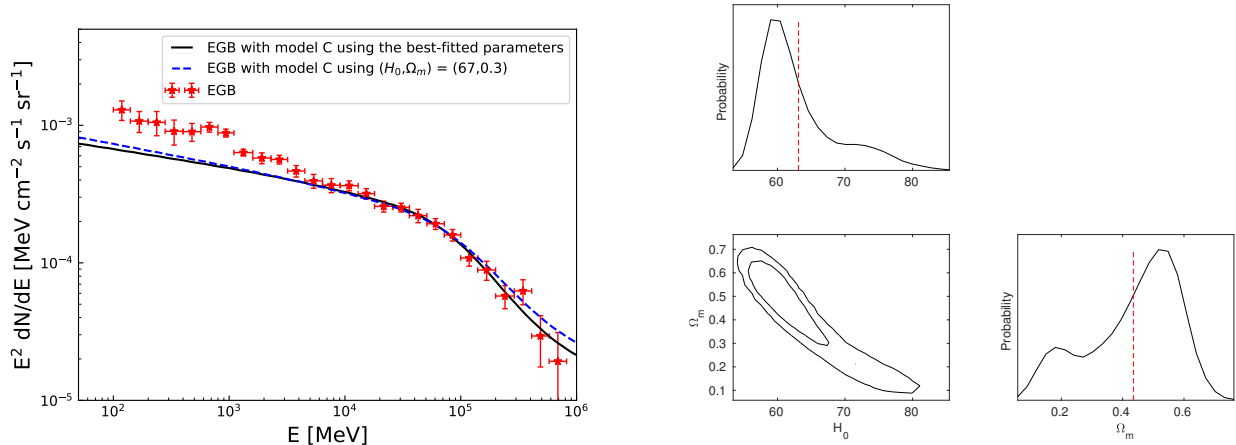


Figure 4. Same as Fig. 3, but with the EBL *Model C*.

REFERENCES

- Abdollahi, S., Ackermann, M., Ajello, M., et al. 2018, *Science*, 362, 1031
- Ackermann, M., Ajello, M., Albert, A., et al. 2015, *ApJ*, 799, 86
- Ackermann, M., Ajello, M., Albert, A., et al. 2016, *PhRvL*, 116, 151105
- Ajello, M., Gasparrini, D., Sánchez-Conde, M., et al. 2015, *ApJL*, 800, L27
- Baldry, I. K., & Glazebrook, K. 2003, *ApJ*, 593, 258
- Barrau, A., Gorecki, A., & Grain, J. 2008, *MNRAS*, 389, 919
- Biteau, J., & Williams, D. A. 2015, *ApJ*, 812, 60
- Blanch, O., & Martinez, M. 2005, *Astroparticle Physics*, 23, 588
- Cole, S., Norberg, P., Baugh, C. M., et al. 2001, *MNRAS*, 326, 255
- Desai, A., Helgason, K., Ajello, M., et al. 2019, *ApJL*, 874, L7
- Domínguez, A., Primack, J. R., Rosario, D. J., et al. 2011, *MNRAS*, 410, 2556
- Domínguez, A., Finke, J., Prada, F., et al., 2013, *ApJ*, 770, 73
- Domínguez, A., & Prada, F. 2013, *ApJL*, 771, L34
- Domínguez, A., Wojtak, R., Finke, J., et al., 2019, arXiv: 1903.12097
- Finke, J. D., Razzaque, S., & Dermer, C. D. 2010, *ApJ*, 712, 238
- Gould, R. J., & Shröder, G. P. 1967, *Phys. Rev.*, 155, 1404

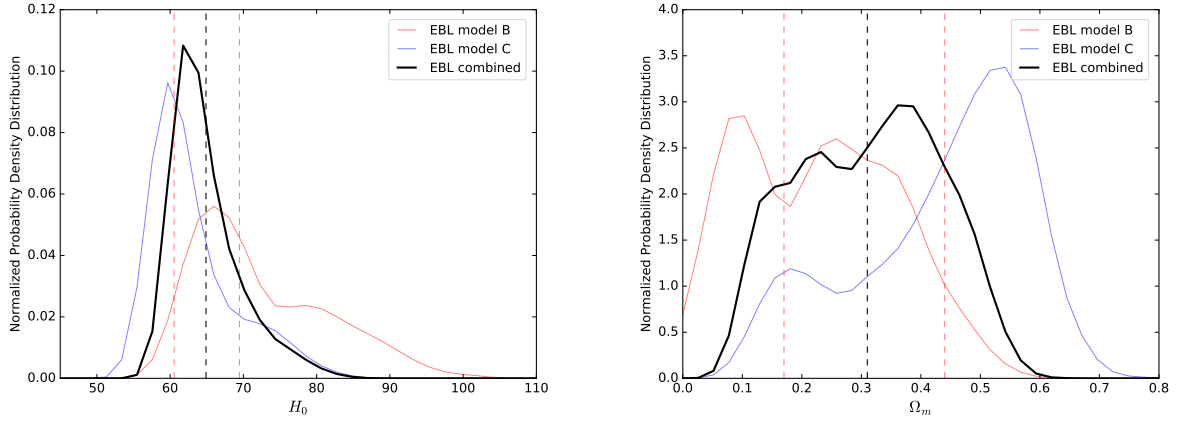


Figure 5. Combined results for H_0 and Ω_m (black solid line). The blue and orange solid lines are the results with the EBL *Model C* and *Model B*, respectively. Vertical dashed lines are the mean (black) and 1σ limits (red) of the combined results. The two models are considered equally likely.

Hopkins, A. M., & Beacom, J. F. 2006, *ApJ*, 651, 142
Mannheim, K. 1996, *RvMA*, 9, 17
Razzaque, S., Dermer, C. D., & Finke, J. D. 2009, *ApJ*, 697, 483
Riess, A. G., Casertano, S., Yuan, W., et al. 2018, *ApJ*, 861, 126
Salamon, M. H., Stecker, F. W., & de Jager, O. C. 1994, *ApJL*, 423, L1

Salpeter, E. E. 1955, *ApJ*, 121, 161
Suyu, S. H., Treu, T., Blandford, R. D., et al. 2012, [arXiv:1202.4459](https://arxiv.org/abs/1202.4459)
Yan, D. H., Zhang, L., Yuan, Q., Fan, Z. H., Zeng, H. D., 2013, *ApJ*, 765, 122